Semiconductor Optoelectronic Devices

Introduction to Physics and Simulation

JOACHIM PIPREK
University of California
at Santa Barbara

ACADEMIC PRESS
An imprint of Elsevier Science
Amsterdam Boston London New York Oxford Paris
San Diego San Francisco Singapore Sydney Tokyo

Semiconductor Optoelectronic Devices

Introduction to Physics and Simulation

Semiconductor Optoelectronic Devices

Introduction to Physics and Simulation

JOACHIM PIPREK
University of California at Santa Barbara

ACADEMIC PRESS
An imprint of Elsevier Science

Amsterdam Boston London New York Oxford Paris San Diego San Francisco Singapore Sydney Tokyo

This book is printed on acid-free paper. ♾

Academic Press
An imprint of Elsevier Science
525 B Street, Suite 1900, San Diego, California 92101-4495, USA
http://www.academicpress.com

Academic Press
84 Theobald's Road, London WC1X 8RR, UK
http://www.academicpress.com

Library of Congress Control Number: 2002111026

International Standard Book Number: 0-12-557190-9

PRINTED IN THE UNITED STATES OF AMERICA
02 03 04 05 06 9 8 7 6 5 4 3 2 1

To Lisa

Contents

Preface xi

List of Tables xiii

I Fundamentals 1

1 Introduction to Semiconductors 3
1.1 Electrons, Holes, Photons, and Phonons . . . 3
1.2 Fermi distribution and density of states . . . 5
1.3 Doping . . . 7

2 Electron energy bands 13
2.1 Fundamentals . . . 13
2.1.1 Electron Waves . . . 13
2.1.2 Effective Mass of Electrons and Holes . . . 16
2.1.3 Energy Band Gap . . . 20
2.2 Electronic Band Structure: The $\vec{k} \cdot \vec{\mathbf{p}}$ Method . . . 23
2.2.1 Two-Band Model (Zinc Blende) . . . 24
2.2.2 Strain Effects (Zinc Blende) . . . 27
2.2.3 Three- and Four-Band Models (Zinc Blende) . . . 30
2.2.4 Three-Band Model for Wurtzite Crystals . . . 32
2.3 Quantum Wells . . . 39
2.4 Semiconductor Alloys . . . 43
2.5 Band Offset at Heterointerfaces . . . 43

3 Carrier transport 49
3.1 Drift and Diffusion . . . 49
3.2 *pn*-Junctions . . . 50
3.3 Heterojunctions . . . 51
3.4 Tunneling . . . 54
3.5 Boundary Conditions . . . 56
3.5.1 Insulator–Semiconductor Interface . . . 57
3.5.2 Metal–Semiconductor Contact . . . 58

3.6 Carrier Mobility 61
3.7 Electron–Hole Recombination 67
3.7.1 Radiative Recombination 67
3.7.2 Nonradiative Recombination 68
3.8 Electron–Hole Generation 71
3.8.1 Photon Absorption 71
3.8.2 Impact Ionization 72
3.8.3 Band-to-Band Tunneling 76
3.9 Advanced Transport Models 78
3.9.1 Energy Balance Model 78
3.9.2 Boltzmann Transport Equation 81

4 Optical Waves **83**
4.1 Maxwell's Equations 83
4.2 Dielectric Function 85
4.2.1 Absorption Coefficient 87
4.2.2 Index of Refraction 91
4.3 Boundary Conditions 94
4.4 Plane Waves 95
4.5 Plane Waves at Interfaces 97
4.6 Multilayer Structures 101
4.7 HelmholtzWave Equations 102
4.8 Symmetric Planar Waveguides 104
4.9 Rectangular Waveguides 108
4.10 Facet Reflection of Waveguide Modes 110
4.11 Periodic Structures 112
4.12 Gaussian Beams 114
4.13 Far Field 116

5 Photon Generation **121**
5.1 Optical Gain 121
5.1.1 Transition Matrix Element 124
5.1.2 Transition Energy Broadening 127
5.1.3 Strain Effects 131
5.1.4 Many-Body Effects 135
5.1.5 Gain Suppression 135
5.2 Spontaneous Emission 136

6 Heat Generation and Dissipation **141**
6.1 Heat Flux Equation 141

6.2 Heat Generation 145
6.2.1 Joule Heat 145
6.2.2 Recombination Heat 145
6.2.3 Thomson Heat 146
6.2.4 Optical Absorption Heat 146
6.3 Thermal Resistance 147
6.4 Boundary Conditions 147

II Devices **149**

7 Edge-Emitting Laser **151**
7.1 Introduction 151
7.2 Models and Material Parameters 156
7.2.1 Drift–Diffusion Model 157
7.2.2 Gain Model 158
7.2.3 Optical Model 158
7.3 Cavity Length Effects on Loss Parameters 161
7.4 Slope Efficiency Limitations 162
7.5 Temperature Effects on Laser Performance 164

8 Vertical-Cavity Laser **171**
8.1 Introduction 171
8.2 Long-Wavelength Vertical-Cavity Lasers 171
8.3 Model and Parameters 174
8.4 Carrier Transport Effects 175
8.5 Thermal Analysis 178
8.6 Optical Simulation 181
8.7 Temperature Effects on the Optical Gain 184

9 Nitride Light Emitters **187**
9.1 Introduction 187
9.2 Nitride Material Properties 188
9.2.1 Carrier Transport 188
9.2.2 Energy Bands 191
9.2.3 Polarization 192
9.2.4 Refractive Index 194
9.2.5 Thermal Conductivity 195
9.3 InGaN/GaN Light-Emitting Diode 196
9.3.1 Device Structure 196
9.3.2 Polarization Effects 197

9.3.3 Current Crowding 198
9.3.4 Quantum Efficiency 200
9.4 InGaN/GaN Laser Diode 204
9.4.1 Device Structure 204
9.4.2 Optical Gain 204
9.4.3 Comparison to Measurements 205
9.4.4 Power Limitations 208
9.4.5 Performance Optimization 210

10 Electroabsorption Modulator 213
10.1 Introduction 213
10.2 Multiquantum Well Active Region 214
10.3 Optical Waveguide 217
10.4 Transmission Analysis 220

11 Amplification Photodetector 227
11.1 Introduction 227
11.2 Device Structure and Material Properties 228
11.3 Waveguide Mode Analysis 232
11.4 Detector Responsivity 234

A Constants and Units 237
A.1 Physical Constants 237
A.2 Unit Conversion 237

B Basic Mathematical Relations 239
B.1 Coordinate Systems 239
B.2 Vector and Matrix Analysis 240
B.3 Complex Numbers 241
B.4 Bessel Functions 242
B.5 Fourier Transformation 243

C Symbols and Abbreviations 245

Bibliography 251

Index 273

Preface

Optoelectronics has become an important part of our lives. Wherever light is used to transmit information, tiny semiconductor devices are needed to transfer electrical current into optical signals and vice versa. Examples include light-emitting diodes in radios and other appliances, photodetectors in elevator doors and digital cameras, and laser diodes that transmit phone calls through glass fibers. Such optoelectronic devices take advantage of sophisticated interactions between electrons and light. Nanometer scale semiconductor structures are often at the heart of modern optoelectronic devices. Their shrinking size and increasing complexity make computer simulation an important tool for designing better devices that meet ever-rising performance requirements. The current need to apply advanced design software in optoelectronics follows the trend observed in the 1980s with simulation software for silicon devices. Today, software for technology computer-aided design (TCAD) and electronic design automation (EDA) represents a fundamental part of the silicon industry. In optoelectronics, advanced commercial device software has emerged, and it is expected to play an increasingly important role in the near future.

The target audience of this book is students, engineers, and researchers who are interested in using high-end software tools to design and analyze semiconductor optoelectronic devices. The first part of the book provides fundamental knowledge in semiconductor physics and in waveguide optics. Optoelectronics combines electronics and photonics and the book addresses readers approaching the field from either side. The text is written at an introductory level, requiring only a basic background in solid state physics and optics. Material properties and corresponding mathematical models are covered for a wide selection of semiconductors used in optoelectronics. The second part of the book investigates modern optoelectronic devices, including light-emitting diodes, edge-emitting lasers, vertical-cavity lasers, electroabsorption modulators, and a novel combination of amplifier and photodetector. InP-, GaAs-, and GaN-based devices are analyzed. The calibration of model parameters using available measurements is emphasized in order to obtain realistic results. These real-world simulation examples give new insight into device physics that is hard to gain without numerical modeling. Most simulations in this book employ the commercial software suite developed by Crosslight Software, Inc. (APSYS, LASTIP, PICS3D). Interested readers can obtain a free trial version of this software including example input files on the Internet at http://www.crosslight.com.

I would like to thank all my students in Germany, Sweden, Great Britain, Taiwan, Canada, and the United States, for their interest in this field and for all their questions, which eventually motivated me to write this book. I am grateful to Dr. Simon Li for creating the Crosslight software suite and for supporting my work. Prof. John Bowers gave me the opportunity to participate in several leading edge research projects, which provided some of the device examples in this book. I am also thankful to Prof. Shuji Nakamura for valuable discussions on the nitride devices. Parts of the manuscript have been reviewed by colleagues and friends, and I would like to acknowledge helpful comments from Dr. Justin Hodiak, Dr. Monica Hansen, Dr. Hans-Jürgen Wünsche, Daniel Lasaosa, Dr. Donato Pasquariello, and Dr. Lisa Chieffo. I appreciate especially the extensive suggestions I received from Dr. Hans Wenzel who carefully reviewed part I of the book.

Writing this book was part of my ongoing commitment to build bridges between theoretical and experimental research. I encourage readers to send comments by e-mail to piprek@ieee.org and I will continue to provide additional help and information at my web site http://www.engr.ucsb.edu/~piprek.

Joachim Piprek
Santa Barbara, California

List of Tables

1.1 Energy Band Gap E_g, Density-of-States Effective Masses m_c and m_v, Effective Densities of States N_c and N_v, and Intrinsic Carrier Concentration n_i at Room Temperature [1, 2, 3, 4, 5, 6, 7] 8

2.1 Electron Effective Masses m_c in Units of m_0 for Conduction Band Minima in Cubic Semiconductors at Low Temperatures [2, 13] . . 18
2.2 Hole Effective Masses in Units of m_0 for the Heavy-Hole Band (m_{hh}), the Light-Hole Band (m_{lh}), and the Split-Off Band (m_{so}) at Room Temperature [1, 2, 4, 5, 6] 21
2.3 Energy Band Gaps at $T = 0$ K and Varshni Parameters of Eq. (2.10) [2, 13, 15] 22
2.4 Fundamental Energy Band Gap at $T = 0$ K (Type Given in Parentheses) and Pässler Parameters of Eq. (2.11) for Cubic Semiconductors [16] 23
2.5 Luttinger Parameters γ for Cubic Semiconductors at Low Temperatures [2, 13] 25
2.6 Lattice Constant a_0, Thermal Expansion Coefficient da_0/dT, Elastic Stiffness Constants C_{11} and C_{12}, and Deformation Potentials b, a_v, a_c for Cubic Semiconductors at Room Temperature [1, 2, 13, 23] 29
2.7 Electron Band-Structure Parameters for Nitride Wurtzite Semiconductors at Room Temperature [13, 16, 29, 31, 32, 33, 34, 35, 36, 37, 38] 35
2.8 Bowing Parameter in Eq. (2.108) for Energy Gaps E_g^Γ, E_g^X, E_g^L, Valence Band Edge E_v^0, and Spin–Orbit Splitting Δ_0 at Room Temperature [13, 42, 43] 44
2.9 Valence Band Edge Reference Level E_v^0 [13], Split-Off Energy Δ_0 [13, 23], Average Valence Band Energy $E_{v,av}^0$ [23], and Electron Affinity χ_0 [46] for Unstrained Cubic Semiconductors 47

3.1 Work functions Φ_M of Selected Metals in Electron Volts (eV) [55] 59
3.2 Mobility Model Parameters of Eqs. (3.27) and (3.28) at Room Temperature 63
3.2 (*Continued*) 64

3.3 Parameters for High-Field Mobility Models (Eqs. (3.29), (3.30), and (3.31)) [4, 56, 68, 69] . . . 66
3.4 Impact Ionization Parameters of Eq. (3.52) at Room Temperature . 74
3.5 Impact Ionization Parameters of Eq. (3.53) at Room Temperature [81] . . . 74
3.6 Impact Ionization Parameters for Electrons: High-Field Room-Temperature Mean Free Path λ_n, Low-Temperature Optical Phonon Energy E^0_{OP}, and Ionization Threshold Energy E^I_n [9] . . . 75

4.1 Parameters s_i and λ_i of the Sellmeier Refractive Index Model for Undoped Semiconductors at Room Temperature (Eq. (4.28)) [104] 91
4.2 Parameters for the Simplified Adachi Model for the Refractive Index below the Band Gap ($\hbar\omega < E_g$) as Given in Eqs. (4.31) [43] and (4.34) [112, 120] . . . 93
4.3 Static ($\varepsilon_{\mathrm{st}}$) and Optical ($\varepsilon_{\mathrm{opt}}$) Dielectric Constants, *Reststrahlen* Wavelength λ_r [99], Band Gap Wavelength λ_g, Refractive Index n_r at Band Gap Wavelength, and Refractive Index Change with Temperature . . . 94

5.1 Energy Parameter E_p of the Bulk Momentum Matrix Element M_b, Correction Factor F_b in Eqs. (5.5) and (2.61) [13], and Longitudinal Optical Phonon Energy $\hbar\omega_{\mathrm{LO}}$ [2, 89] as Used in the Asada Scattering Model (Section 5.1.2) . . . 125

6.1 Crystal Lattice Thermal Conductivity κ_L, Specific Heat C_L, Density ρ_L, Debye Temperature Θ_D, and Temperature Coefficient δ_κ at Room Temperature [1, 3, 6, 38, 46, 69] . . . 142
6.2 Thermal Conductivity Bowing Parameter C_{ABC} (Km/W) in Eqs. (6.7), (6.8), and (6.9) for Ternary Alloys A(B,C) [43, 160] . . 144

7.1 Layer Materials and Room-Temperature Parameters of the MQW Fabry–Perot Laser . . . 155

8.1 Layer Materials and Parameters of the Double-Bonded VCSEL . . 173

9.1 Parameters for the High-Field Electron Mobility Function Given in Eq. (9.2) [63] . . . 190
9.2 Polarization Parameters for Nitride Materials [232] . . . 193
9.3 Layer Structure and Room-Temperature Parameters of the InGaN/GaN LED . . . 196
9.4 Epitaxial Layer Structure and Room-Temperature Parameters of the Nitride Laser . . . 205

10.1 Layer Structure and Parameters of the Electroabsorption Modulator with a Total of 10 Quantum Wells and 11 Barriers . . . 215

11.1 Epitaxial Layer Structure and Parameters of the Amplification Photodetector . . . 229
11.2 Optical Confinement Factors Γ_{amp} and Γ_{det} of the Vertical Modes in Fig. 11.2 for the Amplification and Detection Layers, Respectively . . . 233

Part I

Fundamentals

Chapter 1

Introduction to Semiconductors

This chapter gives a brief introduction to semiconductors. Electrons and holes are carriers of electrical current in semiconductors and they are separated by an energy gap. Photons are the smallest energy packets of light waves and their interaction with electrons is the key physical mechanism in optoelectronic devices. The internal temperature of the semiconductor depends on the energy of lattice vibrations, which can be divided into phonons. The Fermi distribution function for the electron energy and the density of electron states are introduced.

1.1 Electrons, Holes, Photons, and Phonons

Optoelectronics brings together optics and electronics within a single device, a single material. The material of choice needs to allow for the manipulation of light, the manipulation of electrical current, and their interaction. Metals are excellent electrical conductors, but do not allow light to travel inside. Glass and related dielectric materials can accommodate and guide light waves, like in optical fibers, but they are electrical insulators. Semiconductors are in between these two material types, as they can carry electrical current as well as light waves. Even better, semiconductors can be designed to allow for the transformation of light into current and vice versa.

The conduction of electrical current is based on the flow of electrons. Most electrons are attached to single atoms and are not able to move freely. Only some loosely bound electrons are released and become conduction electrons. The same number of positively charged atoms (ions) is left behind; the net charge is zero. The positive charges can also move, as valence electrons jump from atom to atom. Thus, both valence electrons (holes) and conduction electrons are able to carry electrical current. Both the carriers are separated by an energy gap; i.e., valence electrons need to receive at least the gap energy E_g to become conduction electrons. In semiconductors, the gap energy is on the order of 1 eV. The energy can be provided, e.g., by light having a wavelength of less than the gap wavelength

$$\lambda_g = \frac{h\bar{c}}{E_g} \doteq \frac{1240\,\text{nm}}{E_g(\text{eV})} \tag{1.1}$$

with the light velocity c and Planck's constant h. In the wave picture, light is represented by periodic electromagnetic fields with the wavelength λ (see Chapter 4). In the particle picture, light is represented by a stream of energy packets (photons) with the energy

$$E_{\text{ph}} = \frac{hc}{\lambda} = h\nu = \hbar\omega \tag{1.2}$$

(ν is frequency, $\omega = 2\pi\nu$ is angular frequency, and $\hbar = h/2\pi$ is the reduced Planck constant). The photon energy must be at least as large as the band gap E_g to generate electron–hole pairs. Vice versa, conduction electrons can also release energy in the form of light and become valence electrons. This energy exchange between electrons and photons is the key physical mechanism in optoelectronic devices.

From an atomic point of view, valence electrons belong to the outermost electron shell of the atom, which is fully occupied in the case of semiconductors; i.e., no more electrons with the same energy are allowed. As these atoms are joined together in a semiconductor crystal, the electrons start to interact and the valence energy levels separate slightly, forming a valence energy band (Fig. 1.1). Electrons within this band can exchange places but no charge flow is possible unless there is a hole. To generate holes, some electrons must be excited into the next higher energy band, the conduction band, which is initially empty. The concentration n of electrons in the conduction band and the concentration p of holes in the valence band control the electrical conductivity σ of semiconductors

$$\sigma = qn\mu_n + qp\mu_p \tag{1.3}$$

with the elementary charge q and the mobility μ_n and μ_p of holes and electrons, respectively.

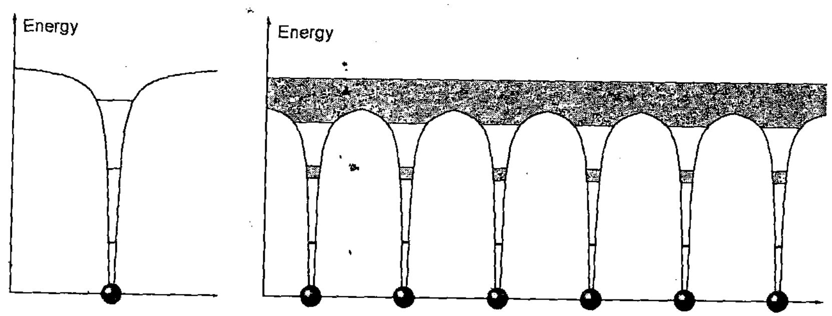

Figure 1.1: Electron energy levels of a single atom (left) become energy bands in a solid crystal (right).

Without external energy supply, the internal temperature T of the semiconductor governs the concentrations n and p. The higher the temperature, the stronger the vibration of the crystal lattice. According to the direction of the atom movement, those vibrations or lattice waves can be classified as follows:

- *longitudinal* (L) waves with atom oscillation in the travel direction of the lattice wave, and
- *transversal* (T) waves with atom oscillation normal to the travel direction.

According to the relative movement of neighbor atoms the lattice waves are

- *acoustic* (A) waves with neighbor atoms moving in the same direction, and
- *optical* (O) waves in ionic crystals with neighbor atoms moving in the opposite direction.

The last type of vibrations interacts directly with light waves as the electric field moves ions with different charges in different directions (see Chapter 4). Phonons represent the smallest energy portion of lattice vibrations, and they can be treated like particles. According to the classification above, four types of phonons are considered: LA, TA, LO, and TO. Electrons and holes can change their energy by generating or absorbing phonons.

1.2 Fermi Distribution and Density of States

The probability of finding an electron at an energy E is given by the Fermi distribution function

$$f(E) = \frac{1}{1 + \exp\left[\frac{E - E_F}{k_B T}\right]} \tag{1.4}$$

with the Fermi energy E_F and the Boltzmann constant k_B ($k_B T \approx 25$ meV at room temperature). At $T = 0$ K, the Fermi energy is the highest electron energy; i.e., it separates occupied from unoccupied energy levels. In pure semiconductors, E_F is typically somewhere in the middle of the band gap (Fig. 1.2). With increasing temperature, more and more electrons are transferred from the valence to the conduction band. The actual concentration of electrons and holes depends on the density of electron states $D(E)$ in both bands. Considering electrons and holes as (quasi-) free particles, the density of states in the conduction and valence band, respectively, becomes a parabolic function of the energy E (Fig. 1.2)

$$D_c(E) = \frac{1}{2\pi^2}\left(\frac{2m_c}{\hbar^2}\right)^{3/2}\sqrt{E - E_c} \quad (E > E_c) \tag{1.5}$$

$$D_v(E) = \frac{1}{2\pi^2}\left(\frac{2m_v}{\hbar^2}\right)^{3/2}\sqrt{E_v - E} \quad (E < E_v) \tag{1.6}$$

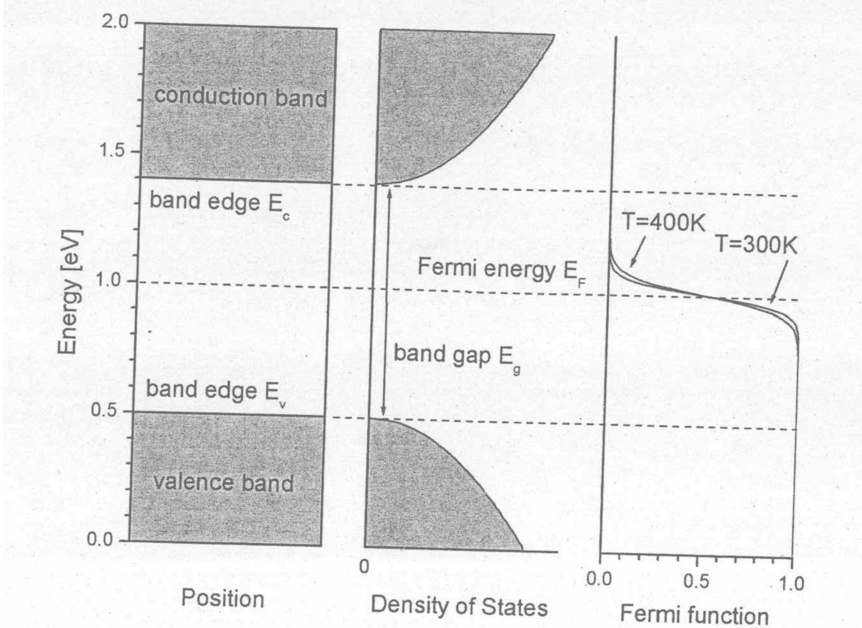

Figure 1.2: Illustration of energy bands, density of states, and Fermi distribution function.

with m_c and m_v being effective masses of electrons and holes, respectively. The carrier density as a function of energy is given by

$$n(E) = D_c(E)f(E) \tag{1.7}$$

$$p(E) = D_v(E)[1 - f(E)]. \tag{1.8}$$

Integration over the energy bands gives the total carrier concentrations

$$n \approx N_c \exp\left(\frac{E_F - E_c}{k_B T}\right) \tag{1.9}$$

$$p \approx N_v \exp\left(\frac{E_v - E_F}{k_B T}\right) \tag{1.10}$$

with the effective density of states

$$N_c = 2\left(\frac{m_c k_B T}{2\pi\hbar^2}\right)^{3/2} \tag{1.11}$$

$$N_v = 2\left(\frac{m_v k_B T}{2\pi\hbar^2}\right)^{3/2} \tag{1.12}$$

for the conduction and valence band, respectively. Equations (1.9) and (1.10) are valid for low carrier concentrations only ($n \ll N_c$, $p \ll N_v$); i.e., with the

Fermi energy separated from the band by more than $3k_BT$, allowing for the Boltzmann approximation

$$f(E) \approx f_B(E) = \exp\left[-\frac{E - E_F}{k_B T}\right]. \tag{1.13}$$

If this condition is satisfied, like in pure (intrinsic) materials, the semiconductor is called nondegenerate. The intrinsic carrier concentration n_i is given as

$$n_i = \sqrt{np} = \sqrt{N_c N_v}\exp\left(-\frac{E_g}{2k_B T}\right). \tag{1.14}$$

At room temperature, n_i is very small in typical semiconductors, resulting in a poor electrical conductivity. Table 1.1 lists n_i and its underlying material parameters for various semiconductors.

Table 1.1: Energy Band Gap E_g, Density-of-States Effective Masses m_c and m_v, Effective Densities of States N_c and N_v, and Intrinsic Carrier Concentration n_i at Room Temperature [1, 2, 3, 4, 5, 6, 7]

Parameter	E_g	m_c	m_v	N_c	N_v	n_i
Unit	**(eV)**	(m_0)	(m_0)	$(10^{18}\ cm^{-3})$	$(10^{18}\ cm^{-3})$	(cm^{-3})
Si (X)	1.12	1.18	0.55	32.2	10.2	7×10^9
Ge (L)	0.66	0.22	0.34	2.6	5.0	1×10^{13}
GaAs (Γ)	1.42	0.063	0.52	0.40	9.41	2×10^6
InP (Γ)	1.34	0.079	0.60	0.56	11.6	1×10^7
AlAs (X)	2.15	0.79	0.80	17.6	18.1	15.
GaSb (Γ)	0.75	0.041	0.82	0.21	18.6	1×10^{12}
AlSb (X)	1.63	0.92	0.98	22.1	24.2	5×10^5
InAs (Γ)	0.36	0.023	0.57	0.09	10.9	9×10^{14}
GaP (X)	2.27	0.79	0.83	17.6	18.9	1.6
AlP (X)	2.45	0.83	0.70	20.0	14.8	0.044
InSb (Γ)	0.17	0.014	0.43	0.04	7.13	2×10^{16}
ZnS (Γ)	3.68	0.34	1.79	4.97	60.3	2×10^{-12}
ZnSe (Γ)	2.71	0.16	0.65	1.61	13.1	8×10^{-5}
CdS (Γ)	2.48	0.21	1.02	2.41	25.7	0.012
CdSe (Γ)	1.75	0.112	1.51	0.94	46.5	1×10^4
CdTe (Γ)	1.43	0.096	0.76	0.75	16.5	3×10^6

Note. Γ, direct semiconductor; X, L, indirect semiconductor; see Fig. 2.6. Parameters for GaN, AlN, and InN are given in Table 2.7.

1.3 Doping

To boost the concentration of electrons or holes, impurity atoms are introduced into the semiconductor crystal. As illustrated in Fig. 1.3, those dopants have energy levels slightly above the valence band (acceptors) or slightly below the conduction band (donors). Acceptors receive an additional electron from the valence band and become negatively charged ions, thereby generating a hole (p-doping). Donors release an electron into the conduction band and become positively charged ions (n-doping). Equation (1.14) is still valid in thermal equilibrium; however, the minority carrier concentration is now much smaller than the concentration of majority carriers. In other words, the Fermi level E_F is close to the majority carrier band edge (Fig. 1.4), and the Boltzmann approximation of Eqs. (1.9) and (1.10) is not valid any more (degenerate semiconductor). In Fermi statistics, the general expressions for the carrier concentrations are

$$n = N_c F_{1/2}\left(\frac{E_F - E_c}{k_B T}\right) \tag{1.15}$$

$$p = N_v F_{1/2}\left(\frac{E_v - E_F}{k_B T}\right), \tag{1.16}$$

where $F_{1/2}$ is the Fermi integral of order one-half, as obtained by integrating Eq. (1.7) or (1.8). Figure 1.5 plots Eq. (1.15) for GaAs as a function of $E_F - E_c$

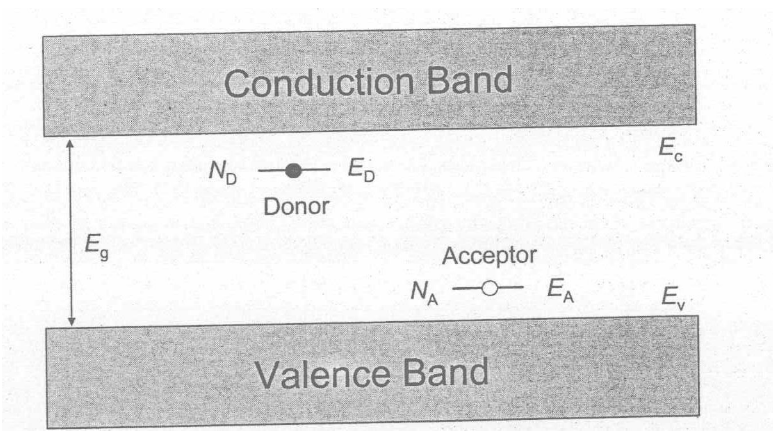

Figure 1.3: Illustration of donor and acceptor levels within the energy band gap (N_D, N_A, concentration; E_D, E_A, energy).

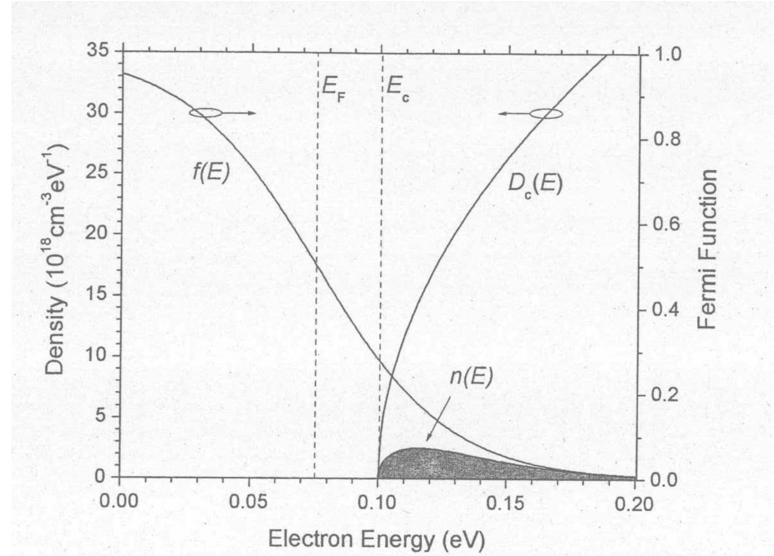

Figure 1.4: Parabolic density of energy band states $D(E)$ of GaAs (Eq. (1.5)) and Fermi distribution $f(E)$ with the Fermi level E_F slightly below the conduction band edge E_c. The gray area gives the carrier distribution $n(E)$ according to Eq. (1.7).

in comparison to the Boltzmann approximation (Eq. (1.9)). Increasing differences can be recognized as the Fermi level approaches the band edge. For numerical evaluation, the following approximation is often used for the Fermi integral and is indicated by the dots in Fig. 1.5 [8]:

$$F_{1/2}^{-1}(x) \approx e^{-x} + \frac{3}{4}\sqrt{\pi}\left\{x^4 + 50 + 33.6x \times \left[1 - 0.68\exp(-0.17(x+1)^2)\right]\right\}^{-3/8}. \tag{1.17}$$

For bulk semiconductors in thermal equilibrium, the actual position of the Fermi level E_F is determined by the charge neutrality condition

$$p + p_D = n + n_A, \tag{1.18}$$

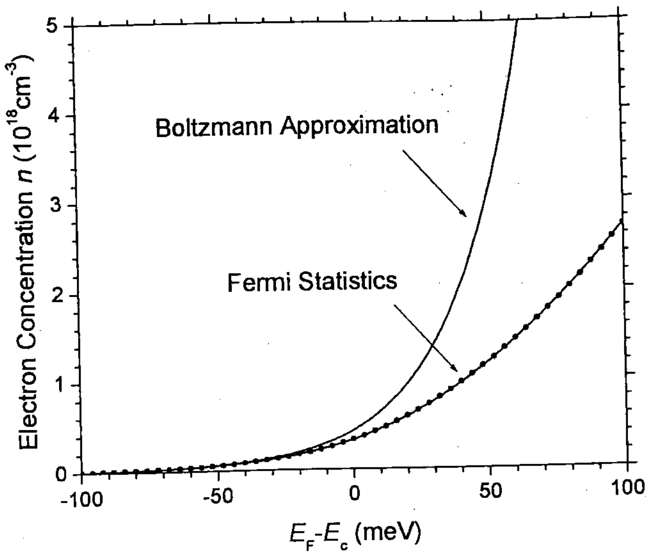

Figure 1.5: Electron concentration in the GaAs conduction band as a function of Fermi level position at room temperature. The result of the exact Fermi integral (Eq. (1.15)) is compared to the approximation by Eq. (1.17) (dots) and to the Boltzmann approximation (Eq. (1.9)).

where p_D is the concentration of ionized donors (charged positive) and n_A is the concentration of ionized acceptors (charged negative)

$$p_D = N_D \left\{ 1 + g_D \exp\left[\frac{E_F - E_D}{k_B T}\right]\right\}^{-1} \tag{1.19}$$

$$n_A = N_A \left\{ 1 + g_A \exp\left[\frac{E_A - E_F}{k_B T}\right]\right\}^{-1}. \tag{1.20}$$

Typical dopant degeneracy numbers are $g_D = 2$ and $g_A = 4$ [9]. E_D and E_A are the dopant energies (Fig. 1.3). Figure 1.6 plots the Fermi level position for n-doping or p-doping versus dopant concentration, as calculated from Eq. (1.18) for GaAs at room temperature. The Fermi level penetrates the conduction band with high n-doping and low ionization energy ($E_D = E_c - 0.01$ eV).

Nonequilibrium carrier distributions can be generated, for instance, by external carrier injection or by absorption of light. In such cases, electron and hole concentrations may be well above the equilibrium level. Each carrier distribution can still be characterized by Fermi functions, but with separate quasi-Fermi levels E_{Fn} and E_{Fp} for electrons and holes, respectively (see Section 3.2).

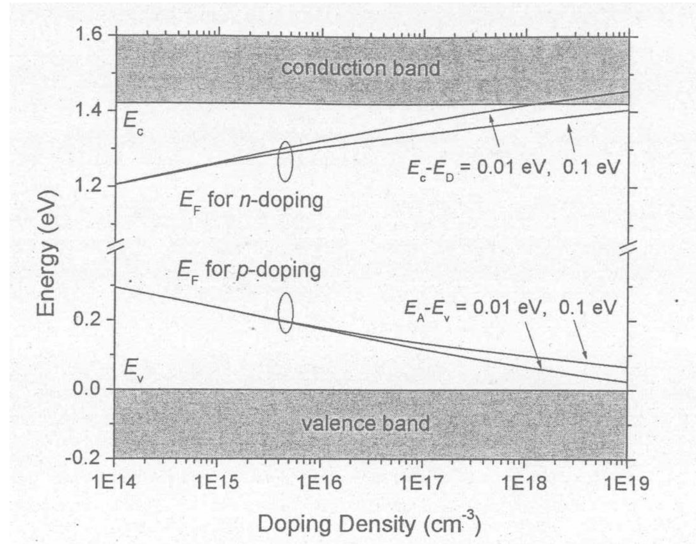

Figure 1.6: GaAs Fermi level E_F as a function of doping density for n-doping or p-doping with the ionization energy E_D and E_A as parameter ($T = 300$ K).

Further Reading

- R. E. Hummel, *Electronic Properties of Materials*, 2nd ed., Springer-Verlag, Berlin, 1993.
- S. M. Sze, *Physics of Semiconductor Devices*, 2nd ed., Wiley, New York, 1981.

Chapter 2

Electron Energy Bands

This is a brief survey of important terms and theories related to the energy bands in semiconductors. First, the fundamental concepts of electron wave vectors $\vec{k}$, energy dispersion $E(\vec{k})$, and effective masses are introduced. Section 2.2 is mathematically more involved as it outlines the $\vec{k} \cdot \vec{\mathbf{p}}$ method, which is most popular in optoelectronics for calculating the band structure. Semiconductor alloys, interfaces of different semiconductor materials, and quantum wells are covered at the end of this chapter.

2.1 Fundamentals

2.1.1 Electron Waves

In the classical picture, electrons are particles that follow Newton's laws of mechanics. They are characterized by their mass m_0, their position $\vec{r} = (x, y, z)$, and their velocity $\vec{v}$. However, this intuitive picture is not sufficient for describing the behavior of electrons within solid crystals, where it is more appropriate to consider electrons as waves. The wave–particle duality is one of the fundamental features of quantum mechanics. Using complex numbers, the wave function for a free electron can be written as

$$\psi(\vec{k}, \vec{r}) \propto \exp(i\,\vec{k}\vec{r}) = \cos(\vec{k}\vec{r}) + i\,\sin(\vec{k}\vec{r}) \tag{2.1}$$

with the wave vector $\vec{k} = (k_x, k_y, k_z)$. The wave vector is parallel to the electron momentum $\vec{p}$

$$\vec{k} = \frac{m_0\vec{v}}{\hbar} = \frac{\vec{p}}{\hbar}, \tag{2.2}$$

and it relates to the electron energy E as

$$E = \frac{m_0}{2}v^2 = \frac{p^2}{2m_0} = \frac{\hbar^2 k^2}{2m_0}, \tag{2.3}$$

with $k^2 = k_x^2 + k_y^2 + k_z^2$. Hence, in all three directions, $E(\vec{p})$ and $E(\vec{k})$ are described by a parabola with the free electron mass m_0 as parameter.

Within semiconductors, an electron is exposed to the periodic lattice potential. It no longer behaves like a free particle as its de Broglie wavelength $2\pi/k$ comes close to the lattice constant a_0. The ensuing Bragg reflections prohibit a further acceleration of the electron, resulting in finite energy ranges for electrons, the energy bands.

In general, electron wave functions need to satisfy the Schrödinger equation

$$\frac{\hbar}{2m_0}\nabla^2\psi - V(\vec{r})\psi = E\psi, \tag{2.4}$$

where the potential $V(\vec{r})$ represents the periodic semiconductor crystal. This equation is often written as

$$H\psi = E\psi \tag{2.5}$$

with H called the Hamiltonian. The Schrödinger equation is for just one electron; all other electrons and atomic nuclei are included in the potential $V(\vec{r})$.[1] For the free electron, $V(\vec{r}) = 0$ and the solution to the Schrödinger equation is of the simple form given by Eq. (2.1). Within semiconductors, the solutions to the Schrödinger equation are so-called Bloch functions, which can be expressed as a linear combination of waves

$$\psi_n(\vec{k}, \vec{r}) = u_n(\vec{k}, \vec{r}) \exp(i\vec{k}\vec{r}), \tag{2.6}$$

with the electron band index n. These functions are plane waves with a space-dependent amplitude factor $u_n(\vec{k}, \vec{r})$ that shows lattice periodicity. A one-dimensional schematic representation is given in Fig. 2.1 to indicate the relationship between the lattice potential and the Bloch function. The probability of finding an electron at the position $\vec{r}$ is proportional to $|\psi_n(\vec{r})|^2$.

In some practical cases, exact knowledge of the semiconductor Bloch functions is not required; only the energy dispersion function $E(\vec{k})$ needs to be found. Inserting Eq. (2.6) into Eq. (2.4), we obtain solutions only for certain ranges of the electron energy $E_n(\vec{k})$, the energy bands, which are separated by energy gaps (Fig. 2.2). A general feature of the solutions to the Schrödinger equation is the periodicity of $E_n(\vec{k})$, given in Fig. 2.2a. This figure shows the periodicity in the k_x direction with a period length of $k_x a_0 = 2\pi$; a shift of the solution $E(k_x)$ by $2\pi/a_0$ in k_x represents the same behavior. Any full segment of the periodic representation is a reduced k-vector representation. It is shown for the range $-\pi/a_0 < k_x < \pi/a_0$ in Fig. 2.2c. This k-range is called first Brillouin zone. The same treatment applies to the other two directions in the $\vec{k}$ space. Figure 2.3 illustrates the first Brillouin zone in two dimensions and it indicates several symmetry points. Besides the central Γ point, the zone boundaries exhibit additional symmetry points. The X point

[1] Many-body theories include the other particles explicitely [10].

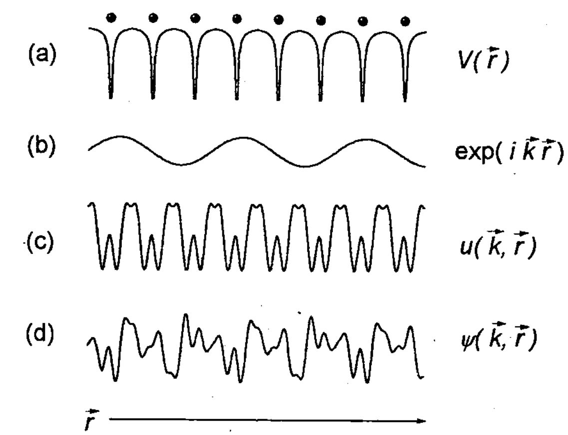

Figure 2.1: Schematic representation of electronic functions in a crystal: (a) potential plotted along a row of atoms, (b) free electron wave function, (c) amplitude factor of Bloch function having the periodicity of the lattice, and (d) Bloch function $\psi = u\exp(ikr)$.

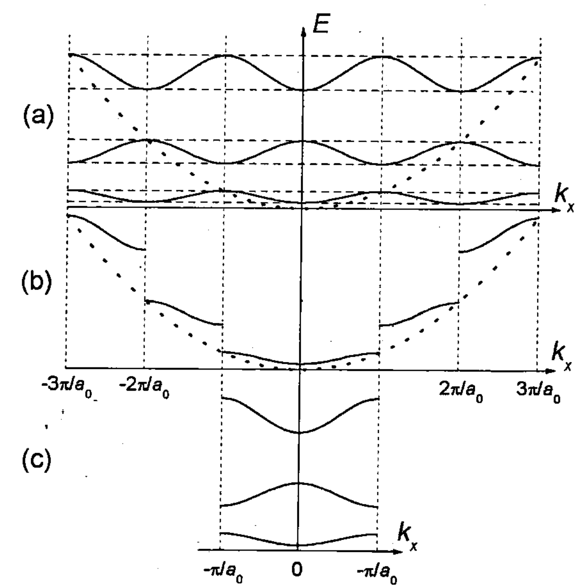

Figure 2.2: Comparison of different representations of the energy dispersion function $E(k)$: (a) periodic, (b) extended wave number, and (c) reduced wave number representation (a_0, lattice constant).